GEOLOGY

Monsoonal control on a delayed response of sedimentation to the 2008 Wenchuan earthquake

Fei Zhang[1,2], Zhangdong Jin[1,2,3]*, A. Joshua West[4], Zhisheng An[1,2], Robert G. Hilton[5], Jin Wang[1,5], Gen Li[4], Alexander L. Densmore[5], Jimin Yu[6,7], Xiaoke Qiang[1,2,8], Youbin Sun[1,2], Liangbo Li[1,9], Longfei Gou[1], Yang Xu[1], Xinwen Xu[10], Xingxing Liu[1], Yanhui Pan[11], Chen-Feng You[12]

Infrequent extreme events such as large earthquakes pose hazards and have lasting impacts on landscapes and biogeochemical cycles. Sediments provide valuable records of past events, but unambiguously identifying event deposits is challenging because of nonlinear sediment transport processes and poor age control. Here, we have been able to directly track the propagation of a tectonic signal into stratigraphy using reservoir sediments from before and after the 2008 Wenchuan earthquake. Cycles in magnetic susceptibility allow us to define a precise annual chronology and identify the timing and nature of the earthquake's sedimentary record. The grain size and Rb/Sr ratio of the sediments responded immediately to the earthquake. However, the changes were muted until 2 years after the event, when intense monsoonal runoff drove accumulation of coarser grains and lower Rb/Sr sediments. The delayed response provides insight into how climatic and tectonic agents interact to control sediment transfer and depositional processes.

INTRODUCTION

Sedimentary archives contain valuable information about past climatic, tectonic, and human activities (*1*–*6*). Abrupt changes in sediment type, volume, and structure, as well as physical, paleontological, geochemical, and mineralogical records, have been used to identify extreme events in the past and to assess how often they occur (*3*–*11*). Sediment pulses that result from earthquake-triggered landslides have been used to reconstruct past events from lake deposits (*12*, *13*), helping to constrain predictive tectonic models and evaluate the long-term effects of large earthquakes (*14*–*16*). However, inferences from sedimentary records are often based on the coincidence of sedimentary changes with indications (e.g., biological or geochemical) of an extreme event. The infrequency of these events means that direct observations are scarce, and the challenges in developing a precise sedimentary chronology at an annual time scale typically preclude direct age assignments for specific event layers (*6*, *10*, *11*, *14*). These obstacles have inhibited full understanding of the depositional processes associated with sediment inputs triggered by extreme events and, particularly, how the event record might be modulated by climate. These interactions as manifest following individual events are also important for understanding the roles of climate and tectonics in controlling erosion, sediment transfer, and landscape evolution (*1*, *17*–*19*).

A unique opportunity to document the link between a large earthquake and its sedimentary signature is provided by continuously deposited and annually resolved sediments from the Zipingpu reservoir in Sichuan Province, China. The reservoir, behind a 156-m-high dam completed in September 2004, is fed by the Min Jiang River (with a drainage area of 22,664 km^2) and is located downstream of the area affected by the 2008 moment magnitude (M_w) 7.9 Wenchuan earthquake (Fig. 1). This devastating earthquake occurred along the steep Longmen Shan mountain front at the eastern margin of the Tibetan Plateau and triggered more than 56,000 landslides in a region with limited landslide activity before the earthquake (*20*, *21*). The total volume of earthquake-triggered landslides was estimated at ~2.8 km^3 (*21*), with a mass (~7.4 Gt) up to four to seven times the total annual sediment export from the Himalayas (1 to 2 Gt) (*22*), using a density of landslide material of 2.65 g/cm^3. The co- and postseismic landslides associated with the Wenchuan earthquake caused substantial changes to the rates of erosion and fluvial sediment transfer (*23*–*25*), as well as to geochemical fluxes (*26*) from the Longmen Shan. The Zipingpu reservoir is ideally located to record the delivery of earthquake-triggered landslide material and document the propagation of the signal from a major earthquake into a sedimentary archive.

Zipingpu reservoir core

In October 2016, a 10.89-m-long sediment core was retrieved from the central area of the Zipingpu reservoir with 100% recovery. The core reached the prereservoir riverbed, characterized by brown coarse sands and gravels. The reservoir sediments mainly consist of horizontally laminated grayish brown silt and clay. The cores were scanned for both magnetic susceptibility (MS) and elemental intensity using an Avaatech x-ray fluorescence (XRF) core scanner. Grain size and magnetic mineralogy were measured on sediment samples using a Malvern 2000 particle size analyzer and an MFK1-FA Kappabridge and vibrating sample magnetometer (VSM), respectively (see Materials and Methods).

[1]SKLLQG, Institute of Earth Environment, Chinese Academy of Sciences, Xi'an 710061, China. [2]CAS Center for Excellence in Quaternary Science and Global Change, Xi'an 710061, China. [3]Institute of Global Environmental Change, Xi'an Jiaotong University, Xi'an 710049, China. [4]Department of Earth Sciences, University of Southern California, Los Angeles, CA 90089, USA. [5]Department of Geography, Durham University, Durham DH1 3LE, UK. [6]Research School of Earth Sciences, The Australian National University, Canberra ACT 2601, Australia. [7]Open Studio for Oceanic-Continental Climate and Environment Changes, Qingdao National Laboratory for Marine Science and Technology, Qingdao 266061, China. [8]School of Environmental Science and Engineering, Chang'an University, Xi'an 710054, China. [9]Interdisciplinary Research Center of Earth Science Frontier, Beijing Normal University, Beijing 100875, China. [10]Shaanxi Key Laboratory of Earth Surface System and Environmental Carrying Capacity, Northwest University, Xi'an 710127, China. [11]MOE Key Laboratory of Western China's Environment Systems, Lanzhou University, Lanzhou 730000, China. [12]EDSRC, Taiwan Cheng Kung University, Tainan 70101, Taiwan.
*Corresponding author. Email: zhdjin@ieecas.cn

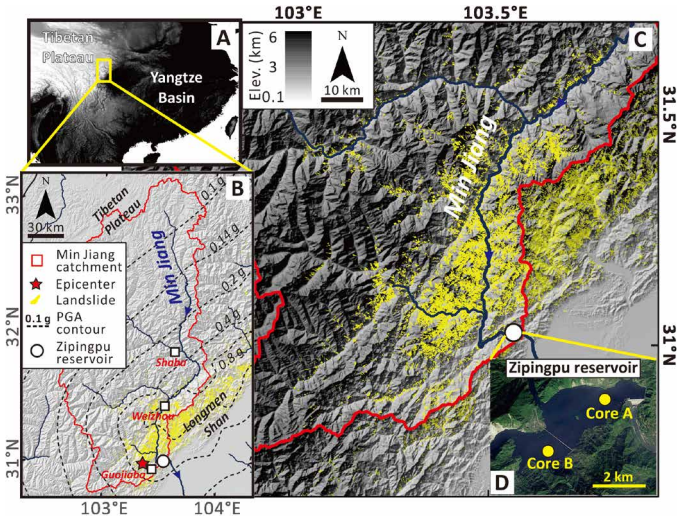

Fig. 1. Map of the core site at the Zipingpu reservoir, the Min Jiang River draining the Longmen Shan mountains, and the landslides triggered by the 2008 M_w 7.9 Wenchuan earthquake. (**A**) Study area in the regional context of the Tibetan Plateau and the Yangtze Basin. (**B**) Map of the Min Jiang catchment (red-outlined polygon) showing earthquake-triggered landslides (*21*) (yellow polygons), earthquake epicenter (red star), peak ground acceleration (PGA) contours (dashed lines), the Zipingpu reservoir (white circle), and the sites of the Weizhou, Shaba, and Guojiaba hydrological stations (white squares). (**C**) The core site at the Zipingpu reservoir (white circle) and landslides (*21*) (yellow polygons). (**D**) The locations of cores A and B at the Zipingpu reservoir.

We interpret the results from the analysis of this core in the context of extensive hydrometeorological data for the region and particularly the well-characterized discharge record of the Min Jiang River. The climate of the region is dominated by the Asian and Indian summer monsoons (*23*), with 82% of annual precipitation occurring from May to October (392 to 1968 mm/year from 2006 to 2016 based on data from six meteorological stations). The annual water discharge of the Min Jiang River (recorded at the Weizhou hydrological station, ~55 km upstream of the reservoir; Fig. 1) averaged 9.47×10^9 m^3/year from 2006 to 2016, with notable interannual variability.

RESULTS

High-resolution chronology from cycles in MS

Cycles in MS are distinct in the Zipingpu core (Fig. 2). Magnetic minerals throughout the core are dominated by magnetite and hematite, whose concentrations determine MS variation (figs. S1 and S2). At the time of the coring (October 2016), MS of the surface sediments was relatively low, corresponding to a high water level (an elevation of ~870 m above sea level) in the reservoir at that time. We attribute low MS values (i.e., low concentrations of magnetic minerals) to an increased distance at high water levels between the coring site and the location of sediment input to the reservoir at the river mouth, compared with that at low water levels (fig. S3). This distance would reduce the accumulation rate of dense magnetic minerals (relative to less dense silicate and carbonate phases) at the coring site at times of high water levels in the reservoir and vice versa. Supporting our interpretation of transport distance as a control on MS, we observe systematically higher MS of surface sediments in the reservoir close to the river mouth compared to the coring site further downstream (fig. S4).

Each year, there are two high water level intervals in the reservoir, resulting from flow regulation at the dam. These high levels consistently correspond to the accumulation of low-MS sediments at the coring site (Fig. 2). On the basis of this inference, we developed an age model for the upper 8.70 m of the core based on the correlation between MS and reservoir water level (Fig. 2). This age model, invoking two peaks in MS each year, exactly retrieves the timing of reservoir impoundment in September 2004. The boundary associated with the 2008 Wenchuan earthquake is then assigned to the core depth of 6.20 m, which corresponds to an abrupt change in the color of the sediments (Fig. 2). Because the reservoir water level is regulated artificially, the adopted age model is independent of the earthquake timing and of variations in water discharge (Q_w).

The sedimentary signature of the Wenchuan earthquake

Because the distinct cycles of MS and the high sedimentation rate (~74 cm/year) in the core allow precise and independent assignment of the earthquake timing within the sediment, we can directly document the depositional signature of the earthquake. Grain size of fluvially derived sediments is a sensitive indicator of changes in sediment transfer processes (*3*, *12*, *27*–*30*). The median grain size (D_{50}) in the Zipingpu core was relatively low before the earthquake (D_{50} = 9.2 ± 0.6 μm, January 2006 to May 2008), although Q_w was moderately high in 2006 and 2007 (Fig. 3). Grain size shows an immediate change following the 2008 Wenchuan earthquake, with D_{50} coarsening from 9.2 to 11.4 μm (fig. S5). It is known that earthquake-triggered landslides mobilized regolith, loosed surficial material, and bedrock (*31*, *32*), supplying coarser material to river channels (*16*, *33*) where it was subsequently transported downstream (*23*, *34*, *35*). We thus attribute the increase in grain size at the earthquake boundary in the Zipingpu core to the delivery of this landslide material by the Min Jiang River. We also observe a drop in sedimentary Rb/Sr ratios, which likely results from a relative increase in Sr inputs (fig. S6) from fresh minerals (i.e., carbonates) by bedrock landslides (*26*). This immediate response is consistent with observations of changes in active fluvial sediment transport following coseismic landsliding (*23*, *34*–*36*), here documented in the sediments deposited downstream. Grain size and elemental ratios do not show cycles linked to MS, indicating that the management of water level does not affect these sedimentary characteristics in the reservoir.

Delayed response of the sedimentary signal from the earthquake

Although we see a distinct sedimentary signal immediately after the Wenchuan earthquake, the most pronounced response in both grain size and Rb/Sr ratio appeared in 2010, 2 years after the earthquake (Fig. 3). In 2010, the D_{50} sharply increased to a maximum of 24.2 μm, while Rb/Sr ratios dropped to their lowest values in the entire core of ~0.35. This delayed response likely reflects the discharge dynamics of the Min Jiang River; 2008 and 2009 had relatively lower peak Q_w and thus lower fluvial transport capacity than other years (Fig. 3), inhibiting the transfer of earthquake-triggered landslide sediment to the reservoir. The peak Q_w in 2010 was much higher, with intense rainstorms that caused extensive debris flows (*37*), flooded Yingxiu town upstream of the reservoir, and resulted in >8000 resident evacuations (*32*). Both grain size and Rb/Sr ratios remained peaks but variable during 2010 and 2011. The delay of the sedimentary response in the reservoir highlights the importance of hydrological controls on sediment evacuation and downstream delivery following an earthquake, consistent with studies of suspended sediment

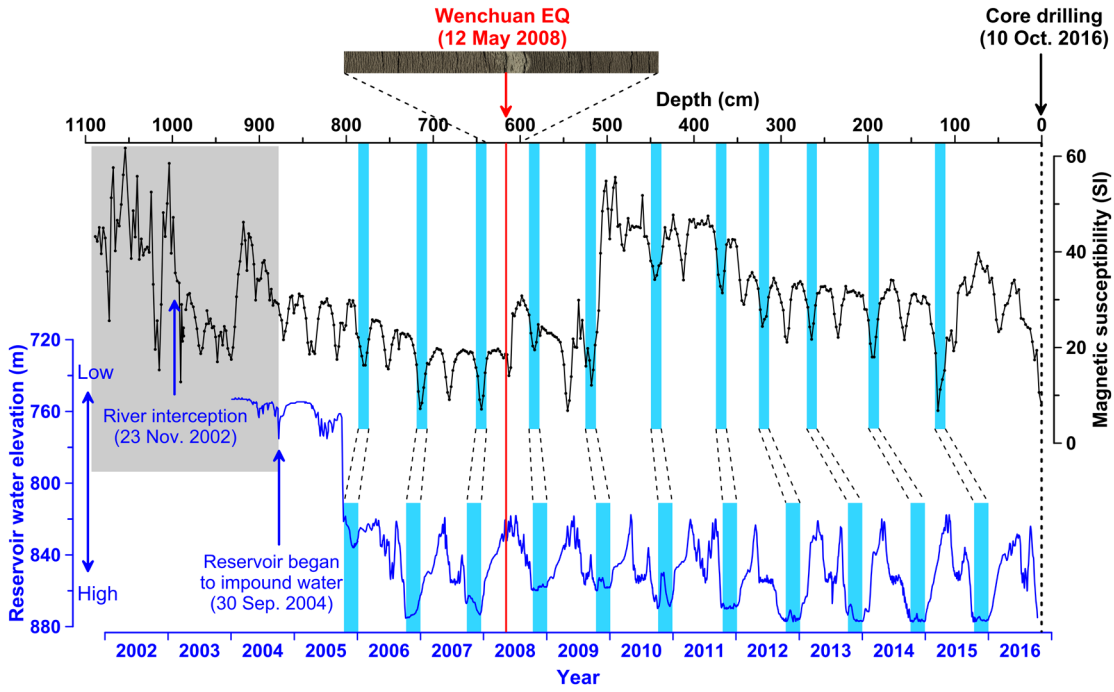

Fig. 2. Chronology of the Zipingpu reservoir sediment core based on the correlation between reservoir water level and sedimentary MS. The red line marks the boundary of the 2008 Wenchuan earthquake (EQ) in the core; two blue arrows show the dates of river interception (23 November 2002) and water impoundment in the reservoir (30 September 2004). The blue-shaded bars indicate annual high water levels (note inverted scale) that are associated with low MS values. Large variation in MS observed before reservoir impoundment is likely due to water discharge (Q_w) changes determining the transport and deposition of heavy magnetic minerals. The role of Q_w appears to have become highly muted from 2005 onward, with MS instead controlled by reservoir water level. We use this as the basis for our chronology while acknowledging that Q_w may still have had minor effects, for example, influencing secondary features in the MS record and potentially introducing some uncertainties especially at seasonal time scales.

concentrations and fluxes in rivers draining earthquake-affected regions (*23*, *34*, *35*).

Notably, annual reservoir sediment thickness has a statistically significant correlation (r^2 = 0.62) with total annual Q_w (Fig. 4A), further supporting the control of monsoonal precipitation on sediment transfer in this setting. The sedimentation rate at the core site did not change systematically after the earthquake, despite changes in total fluvial sediment fluxes (fig. S7). These observations suggest that sedimentation rate at the core site, which is located at a relatively distal position within the reservoir, has been largely controlled by hydrodynamic conditions rather than upstream sediment supply. Observed changes in grain size and Rb/Sr provenance signatures, but not in sedimentation rate, suggest that sediment grain size and geochemistry may better record events than sediment thickness, at least for conditions similar to the core site studied here.

The relationship between intense runoff in the Min Jiang River and the fraction of coarse grains (>32 μm) in the reservoir sediment was altered by the earthquake (Fig. 4B). The coarse grain fraction increased with intense runoff (r^2 = 0.71) after the earthquake and was consistently higher than limited measurements made before the earthquake (Fig. 4B). This shift in particle size following the earthquake may indicate a change in sediment transfer regime for the >32-μm grains in the Min Jiang River, from "supply-limited" to "transport-limited" regimes (Fig. 4B) (*38*). Under the transport-limited regime, low Q_w in 2009 resulted in limited transfer of coarse grains, whereas in 2010, high Q_w facilitated enhanced sediment transport. The peak in transport capacity in 2010, reflected in the coarse grains in the reservoir core, is further supported by an eightfold increase in sediment yield in a Min Jiang tributary near the earthquake epicenter during that year (fig. S7).

After 2011, both grain size and Rb/Sr ratio returned gradually to pre-earthquake values over a time scale of ~5 to 6 years. However, much of the 2008 Wenchuan earthquake-triggered landslide debris remains visible on hillslopes and in river channels 10 years later (fig. S8). If runoff intensity reaches or exceeds 2010 levels in the future (Fig. 3), then this may create an additional sedimentary response in the reservoir. Quantifying the precise record that is left by time-varying runoff would provide important information for understanding longer-term sedimentary signatures at this location and other tectonically active mountain ranges, such as those observed in the several packages of coarser sediments that have accumulated over decades following earthquake events in New Zealand lake records (*12*).

DISCUSSION

Field data and modeling studies have revealed how sedimentation is regulated by climatic (*1*, *2*, *18*, *28*) and tectonic forcings (*5*, *6*, *12*, *30*, *39*), but the interplay of these factors in creating the sedimentary signatures of an earthquake is typically difficult to observe and quantify directly (*11*, *12*). Our well-dated sediment core with very high sedimentation rates, together with independent hydrometeorological data, enables us to identify the role of hydroclimatic forcing in the creation of a seismic record. The combination of these data in the observational record allows us to decode detailed annual depositional

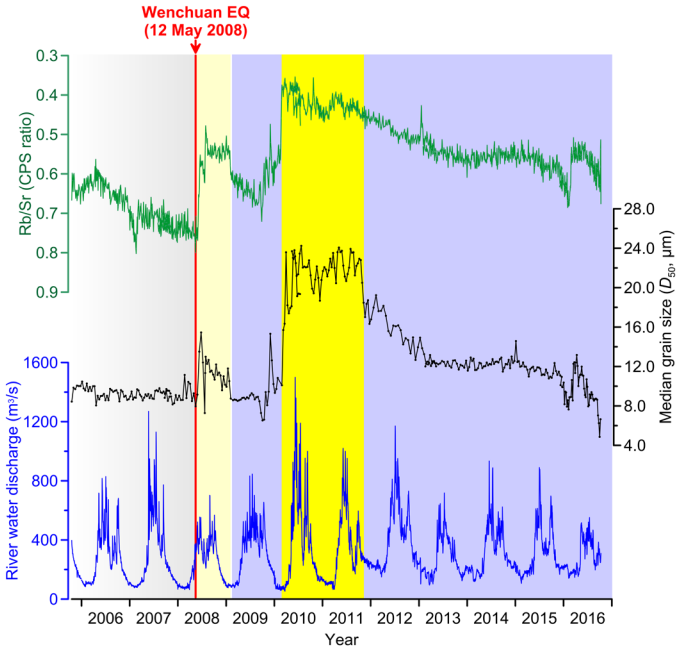

Fig. 3. Core sedimentary data from the Zipingpu reservoir and water discharge (Q_w) in the Min Jiang River before and after the 2008 Wenchuan earthquake. Daily mean river Q_w (blue), median grain size D_{50} (black), and Rb/Sr ratios (green). Red line marks the time of the 2008 Wenchuan earthquake based on independent chronology (Fig. 2). Q_w data are from the main stem of the Min Jiang at the Weizhou hydrological station (Fig. 1) that accounts for more than 70% of the discharge flux to the Zipingpu reservoir. Both Rb/Sr ratio and D_{50} show remarkable changes after the earthquake, with the most pronounced shifts in 2010 associated with very high Q_w. A slight offset in the timing of changes in sediment properties in 2010 appears to precede the rise in Q_w, potentially because of uncertainties in the chronology related to seasonally varying sedimentation rates; the chronology defined by linear interpolation between the low-MS tie points is likely to introduce some uncertainties within a year (Fig. 2) and thus accurately captures the timing of changes at the annual but not at the seasonal scales. CPS, counts per second.

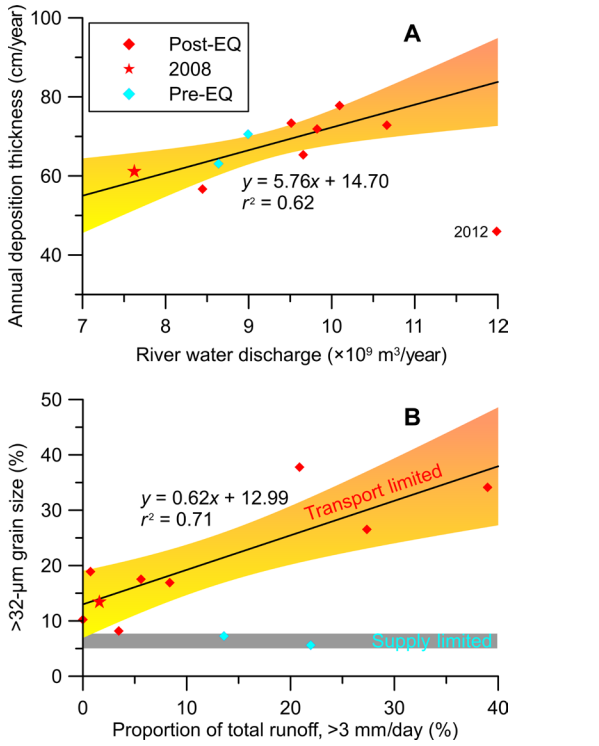

Fig. 4. Sedimentological versus hydrological parameters before and after the 2008 Wenchuan earthquake. Relationships between (**A**) annual water discharge and annual depositional thickness and (**B**) the proportion of total runoff of >3 mm/day and the percentage of coarse grains (>32 μm). Black lines show the best-fit relationship from linear least-squares regression, and the yellow-shaded regions show 95% confidence intervals, excluding the data from 2012 in (A). The outlier from 2012 may result from high Q_w dominated by heavy rainfall in the upstream portions of the Min Jiang River catchment with limited earthquake-triggered landslides (fig. S9). In (B), the relationship may reflect a shift from a supply-limited regime (gray-shaded region) to a transport-limited regime (yellow-shaded region) after the Wenchuan earthquake.

processes associated with a single large earthquake event and, crucially, to assess the role of climate in sediment accumulation under postseismic conditions. Our results also provide modern context for other studies of event deposits, which typically lack the annual chronologic resolution (*6*, *10*–*12*, *14*) needed to resolve the dynamics and evolution of a single event.

The Zipingpu core shows that the sedimentary signal of widespread inputs of landslide debris after an earthquake is likely regulated by runoff associated with the monsoonal climate. Even when a major earthquake has greatly perturbed the system and provided large amounts of landslide material to rivers (*21*, *31*, *34*, *35*), the downstream signal recorded even in fairly proximal sedimentary deposits (such as the mountain-front reservoir studied here) may be muted if fluvial transport capacity is insufficient. This interplay of tectonic and climatic factors may have particular relevance for interpretation and correlation of event deposits between different locations (*6*, *10*–*14*, *18*, *19*). For example, a major earthquake followed by a multiyear period of aridity and low fluvial transport capacity may be difficult to identify in sedimentary deposits and any record will be somewhat lagged, while an earthquake followed by intense rainfall in following years such as after the 1999 M_w 7.9 Chi-Chi earthquake (*34*, *35*) could leave a more distinct and immediate signature.

Our results also show how the hydroclimatic control on sediment transport following an earthquake could generate the appearance of multiple "peaks" in a sedimentary record; for example, the muted change in grain size at the time of the Wenchuan earthquake is followed by a much more prominent peak a few years later, driven by intense rainfall (Fig. 3). In a paleo-archive, these multiple peaks might be mistakenly interpreted as reflecting two different earthquakes (such as a main shock/aftershock sequence or a sequence of earthquakes on adjacent fault segments), emphasizing the need to tease apart the hydroclimatic role in these records for robust interpretation.

Although hydrological filtering of an earthquake event is likely to affect sedimentary records (*16*, *19*, *28*, *29*), it is notable that the seismic signal of the Wenchuan earthquake is propagated quickly and clearly in the sediment grain size and bulk elemental chemistry when evaluated in terms of the typical precision of available geochronological tools (Fig. 3). Efficient transfer of the earthquake signal into reservoir sediments is emphasized by the similar trends shown by suspended sediment yields in the Min Jiang (fig. S7) and the grain-size and geochemical records in the reservoir (Fig. 3). The identifiable fingerprint of the Wenchuan earthquake in fairly proximal mountain-front reservoir sediments shows that fine-grained sedimentary deposits are less susceptible to environmental signal shredding by the nonlinear

filters imposed by sediment transport, when compared to rates of bed load transport (*16*, *19*, *28*, *29*, *40*), which supports views from lacustrine records of landscape responses to large earthquakes (*12*).

The hydrological imprint of a large earthquake on the sedimentary record may also provide information on the sediment-related hazards that can persist for many years after the event, controlled largely by hydroclimatic conditions. Extensive storm-triggered debris flows and landslides had devastating effects in the years following the Wenchuan earthquake, particularly in 2010 (*32*, *37*), and we find that their signature is (perhaps expectedly) recorded in the Zipingpu reservoir. If a characteristic fingerprint of these postseismic sediment pulses could be constrained from sedimentary archives, then this might shed new light on how long the associated hazards can persist (i.e., years, decades, or longer).

Our unique, well-dated sediment core in a man-made reservoir provides greater understanding of how erosion and sedimentation processes respond to an extreme event. Our results emphasize the importance of the interplay between a major earthquake and the prevailing monsoonal climate, highlighting the central role of runoff as an erosional agent in removing earthquake-triggered landslide material and in creating a depositional signal of the earthquake. The high-resolution Zipingpu record provides rare direct evidence that can inform the interpretation of paleorecords and helps to illuminate the ways in which sedimentary archives reflect the complex interaction of tectonics and climate in controlling sediment transfer in tectonically active mountain ranges.

MATERIALS AND METHODS

Zipingpu reservoir and sediment core drilling

The Zipingpu reservoir is located at the Min Jiang River at the Longmen Shan mountain front, upstream of the Sichuan Basin (Fig. 1), with a water depth of 110 m at the highest water level and 57 m at the lowest water level in 2016. The entrance of the reservoir at the highest water level is ~2 km downstream from the epicenter of the 2008 Wenchuan earthquake (fig. S3). The reservoir forms an elongated "L" shape, with a maximum length of ~19 km and a width of ~2.1 km at its highest water level. The location of the reservoir means that it captures a significant portion of the landslide material associated with the 2008 Wenchuan earthquake. According to the records from the Zipingpu Reservoir Company, the Min Jiang River channel was intercepted on 23 November 2002 when dam construction began. The reservoir started to impound water with a maximum water depth of 23 m (an elevation of 775 m) on 30 September 2004, and operations fully began 1 year later, when water level increased abruptly to an elevation of 821 m (a water depth of 69 m near the dam) (Fig. 2). The daily water level has been monitored by the Zipingpu Reservoir Company since 2004. With a view to dam safety and requirements for irrigation during dry seasons, the water level of the reservoir is regulated artificially. There are two periods with high water level each year: The first is during monsoonal rainy season (June and July), although the reservoir is discharged at this time to release the large volume of water received; and the second is during the dry season, when the highest level (an elevation of ~877 m) is achieved from late September to January to ensure adequate agricultural irrigation and drinking water for the following spring (Fig. 2).

In middle October 2016, a 10.89-m-long sediment core ZPP-A (31°02′8.20″N, 103°33′48.20″E, 870 m above sea level) was retrieved using an Austrian UWITEC piston coring platform from the deepest part of the Zipingpu reservoir (Fig. 1) at a water depth of 102.9 m. The core achieved 100% recovery. This core was recovered to the depth of the old river bed where coarse sands and bedrock fragments were observed at the core bottom. The core sediments mainly consisted of horizontally laminated grayish brown silt and clay. The lower 2.19 m was characterized by silt and brown sand layers, with dispersed fine gravel at the bottom (1 to 4 cm in diameter). This interval was considered to have been rapidly deposited before water was impounded in the reservoir and was excluded from our discussion. In addition, a 60-cm-short core (ZPP-B; 31°1′6.30″N, 103°32′28.50″E) was retrieved using a gravity corer at the location of core B, 2.85 km upstream of the core A (Fig. 1 and fig. S3).

Core sediment scanning and analyses

After the cores were split lengthwise, the sediment stratigraphy was photographed and described. The cores were scanned lengthwise along the center of the split core surface using an Avaatech III XRF core scanner for intensities of both chemical elements and MS at the Key Laboratory of Western China's Environmental Systems at Lanzhou University. The element scanning conditions at a resolution of 5 mm were as follows: settings of 30 kV and 2 mA with an x-ray tube, a step size of 5 mm, and an exposure time of 20 s for elements. The signal intensity of each element is expressed as counts per second. MS was scanned every 2 cm with an analytical precision of 0.1 SI using a Bartington Instruments MS2E magnetic susceptibility meter at a frequency of 2 kHz. Sixteen typical samples were chosen for magnetic mineralogy identification using an MFK1-FA Kappabridge and VSM at the Environmental Magnetism Laboratory in the Institute of Earth Environment, Chinese Academy of Sciences (IEECAS) (figs. S1 and S2).

For grain size analyses, a total of 648 samples were collected at 2-cm core intervals. The samples were pretreated by adding 10% H_2O_2 and 10% HCl to remove organic matter, carbonate, and iron oxides and were dispersed with $(NaPO_3)_6$ in an ultrasonic bath before grain size measurement. The grain size distribution was measured by a Malvern 2000 laser diffraction instrument with 100 bins ranging from 0.02 to 2000 μm in the IEECAS. The analytical error of median grain size is better than ~2%, based on repeated measurements of samples.

SUPPLEMENTARY MATERIALS

Supplementary material for this article is available at http://advances.sciencemag.org/cgi/content/full/5/6/eaav7110/DC1

Supplementary Materials and Methods: Magnetic mineralogy

Fig. S1. χ-T curves of representative samples.

Fig. S2. Hysteresis loops of representative samples from the Zipingpu sediment core.

Fig. S3. Seasonal water level difference of the Zipingpu reservoir.

Fig. S4. Difference in MS of topmost 60-cm sediments of cores A and B from the Zipingpu reservoir.

Fig. S5. Grain size distributions of the Zipingpu core sediments around the earthquake.

Fig. S6. Correlation of Rb/Sr ratio versus Sr content.

Fig. S7. Interannual variations of daily runoff (>3 mm/day; orange crosses), daily (gray dots), and annual (blue dots) suspended particulate material yield at the Guojiaba hydrological station on the Shouxi River before and after the Wenchuan earthquake.

Fig. S8. Remaining seismic landslides within the catchment after ten years since the earthquake.

Fig. S9. Difference in suspended sediment fluxes versus river water discharge (Q_w) between two typical tributaries within the Min Jiang Basin during the period of 2006–2012.

References (*41*–*46*)

REFERENCES AND NOTES

1. P. Zhang, P. Molnar, W. R. Downs, Increased sedimentation rates and grain sizes 2–4 Myr ago due to the influence of climate change on erosion rates. *Nature* **410**, 891–897 (2001).

2. J. A. Covault, B. W. Romans, A. Fildani, M. McGann, S. A. Graham, Rapid climatic signal propagation from source to sink in a southern California sediment-routing system. *J. Geol.* **118**, 247–259 (2010).
3. S. E. Munoz, L. Giosan, M. D. Therrell, J. W. Remo, Z. Shen, R. M. Sullivan, C. Wiman, M. O'Donnell, J. P. Donnelly, Climatic control of Mississippi river flood hazard amplified by river engineering. *Nature* **556**, 95–98 (2018).
4. J. D. Sims, Earthquake-induced structures in sediments of Van Norman Lake, San Fernando, California. *Science* **182**, 161–163 (1973).
5. R. Bao, M. Strasser, A. P. McNichol, N. Haghipour, C. McIntyre, G. Wefer, T. I. Eglinton, Tectonically-triggered sediment and carbon export to the Hadal zone. *Nat. Commun.* **9**, 121 (2018).
6. J. Moernaut, M. Van Daele, K. Fontijn, K. Heirman, P. Kempf, M. Pino, G. Valdebenito, R. Urrutia, M. Strasser, M. De Batist, Larger earthquakes recur more periodically: New insights in the megathrust earthquake cycle from lacustrine turbidite records in south-central Chile. *Earth Planet. Sci. Lett.* **481**, 9–19 (2018).
7. R. A. Morton, G. Gelfenbaum, B. E. Jaffe, Physical criteria for distinguishing sandy tsunami and storm deposits using modern examples. *Sediment. Geol.* **200**, 184–207 (2007).
8. G. Einsele, Event deposits: The role of sediment supply and relative sea-level changes—Overview. *Sediment. Geol.* **104**, 11–37 (1996).
9. P. F. Hudson, Event sequence and sediment exhaustion in the lower Panuco Basin, Mexico. *Catena* **52**, 57–76 (2003).
10. K. Kremer, S. B. Wirth, A. Reusch, D. Fäh, B. Bellwald, F. S. Anselmetti, S. Girardclos, M. Strasser, Lake-sediment based paleoseismology: Limitations and perspectives from the Swiss Alps. *Quat. Sci. Rev.* **168**, 1–18 (2017).
11. U. Avşar, A. Hubert-Ferrari, M. D. Batist, N. Fagel, A 3400 year lacustrine paleoseismic record from the North Anatolian Fault, Turkey: Implications for bimodal recurrence behavior. *Geophys. Res. Lett.* **41**, 377–384 (2014).
12. J. D. Howarth, S. J. Fitzsimons, R. J. Norris, G. E. Jacobsen, Lake sediments record cycles of sediment flux driven by large earthquakes on the Alpine fault, New Zealand. *Geology* **40**, 1091–1094 (2012).
13. N. Praet, J. Moernaut, M. Van Daele, E. Boes, P. J. Haeussler, M. Strupler, S. Schmidt, M. G. Loso, M. De Batist, Paleoseismic potential of sublacustrine landslide records in a high-seismicity setting (south-central Alaska). *Mar. Geol.* **384**, 103–119 (2017).
14. M. Schnellmann, F. S. Anselmetti, D. Giardini, J. A. McKenzie, S. N. Ward, Prehistoric earthquake history revealed by lacustrine slump deposits. *Geology* **30**, 1131–1134 (2002).
15. S. Barbot, N. Lapusta, J. P. Avouac, Under the hood of the earthquake machine: Toward predictive modeling of the seismic cycle. *Science* **336**, 707–710 (2012).
16. T. Croissant, D. Lague, P. Steer, P. Davy, Rapid post-seismic landslide evacuation boosted by dynamic river width. *Nat. Geosci.* **10**, 680–684 (2017).
17. K. X. Whipple, The influence of climate on the tectonic evolution of mountain belts. *Nat. Geosci.* **2**, 97–104 (2009).
18. S. E. Harris, A. C. Mix, Climate and tectonic influences on continental erosion of tropical South America, 0–13 Ma. *Geology* **30**, 447–450 (2002).
19. J. J. Armitage, R. A. Duller, A. C. Whittaker, P. A. Allen, Transformation of tectonic and climatic signals from source to sedimentary archive. *Nat. Geosci.* **4**, 231–235 (2011).
20. W. B. Ouimet, Landslides associated with the May 12, 2008 Wenchuan earthquake: Implications for the erosion and tectonic evolution of the Longmen Shan. *Tectonophysics* **491**, 244–252 (2010).
21. G. Li, A. J. West, A. L. Densmore, Z. Jin, R. N. Parker, R. G. Hilton, Seismic mountain building: Landslides associated with the 2008 Wenchuan earthquake in the context of a generalized model for earthquake volume balance. *Geochem. Geophys. Geosyst.* **15**, 833–844 (2014).
22. V. Galy, C. France-Lanord, O. Beyssac, P. Faure, H. Kudrass, F. Palhol, Efficient organic carbon burial in the Bengal fan sustained by the Himalayan erosional system. *Nature* **450**, 407–410 (2007).
23. J. Wang, Z. Jin, R. G. Hilton, F. Zhang, A. L. Densmore, G. Li, A. J. West, Controls on fluvial evacuation of sediment from earthquake-triggered landslides. *Geology* **43**, 115–118 (2015).
24. G. Li, A. J. West, A. L. Densmore, Z. Jin, F. Zhang, J. Wang, M. Clark, R. G. Hilton, Earthquakes drive focused denudation along a tectonically active mountain front. *Earth Planet. Sci. Lett.* **472**, 253–265 (2017).
25. J. Wang, Z. Jin, R. G. Hilton, F. Zhang, G. Li, A. L. Densmore, D. R. Gröcke, X. Xu, A. J. West, Earthquake-triggered increase in biospheric carbon export from a mountain belt. *Geology* **44**, 471–474 (2016).
26. Z. Jin, A. J. West, F. Zhang, Z. An, R. G. Hilton, J. Yu, J. Wang, G. Li, L. Deng, X. Wang, Seismically enhanced solute fluxes in the Yangtze River headwaters following the A.D. 2008 Wenchuan earthquake. *Geology* **44**, 47–50 (2016).
27. E. H. Dingle, H. D. Sinclair, M. Attal, D. T. Milodowski, V. Singh, Subsidence control on river morphology and grain size in the Ganga Plain. *Am. J. Sci.* **316**, 778–812 (2016).
28. M. D'arcy, A. C. Whittaker, D. C. Roda-Boluda, Measuring alluvial fan sensitivity to past climate changes using a self-similarity approach to grain-size fining, Death Valley, California. *Sedimentology* **64**, 388–424 (2017).
29. B. W. Romans, S. Castelltort, J. A. Covault, A. Fildani, J. P. Walsh, Environmental signal propagation in sedimentary systems across timescales. *Earth Sci. Rev.* **153**, 7–29 (2016).
30. A. C. Whittaker, M. Attal, P. A. Allen, Characterising the origin, nature and fate of sediment exported from catchments perturbed by active tectonics. *Basin Res.* **22**, 809–828 (2010).
31. Y. Yin, F. Wang, P. Sun, Landslide hazards triggered by the 2008 Wenchuan earthquake, Sichuan, China. *Landslides* **6**, 139–152 (2009).
32. C. Tang, J. Zhu, J. Ding, X. F. Cui, L. Chen, J. S. Zhang, Catastrophic debris flows triggered by a 14 August 2010 rainfall at the epicenter of the Wenchuan earthquake. *Landslides* **8**, 485–497 (2011).
33. G. Li, A. J. West, A. L. Densmore, D. E. Hammond, Z. Jin, F. Zhang, J. Wang, R. G. Hilton, Connectivity of earthquake-triggered landslides with the fluvial network: Implications for sediment transport after the 2008 Wenchuan earthquake. *J. Geophys. Res.* **121**, 703–724 (2016).
34. N. Hovius, P. Meunier, C. W. Lin, H. Chen, Y. G. Chen, S. Dadson, M. J. Horng, M. Lines, Prolonged seismically induced erosion and the mass balance of a large earthquake. *Earth Planet. Sci. Lett.* **304**, 347–355 (2011).
35. S. J. Dadson, N. Hovius, H. Chen, W. B. Dade, J. C. Lin, M. L. Hsu, C. W. Lin, M. J. Horng, T. C. Chen, J. Milliman, C. P. Stark, Earthquake-triggered increase in sediment delivery from an active mountain belt. *Geology* **32**, 733–736 (2004).
36. T. Koi, N. Hotta, I. Ishigaki, N. Matuzaki, Y. Uchiyama, M. Suzuki, Prolonged impact of earthquake-induced landslides on sediment yield in a mountain watershed: The Tanzawa region, Japan. *Geomorphology* **101**, 692–702 (2008).
37. Q. Xu, S. Zhang, W. L. Li, Th. W. J. Van Asch, The 13 August 2010 catastrophic debris flows after the 2008 Wenchuan earthquake, China. *Nat. Hazards Earth Syst. Sci.* **12**, 201–216 (2012).
38. A. J. West, R. Hetzel, G. Li, Z. Jin, F. Zhang, R. G. Hilton, A. L. Densmore, Dilution of ^{10}Be in detrital quartz by earthquake-induced landslides: Implications for determining denudation rates and potential to provide insights into landslide sediment dynamics. *Earth Planet. Sci. Lett.* **396**, 143–153 (2014).
39. P. A. Allen, P. L. Heller, Dispersal and preservation of tectonically generated alluvial gravels in sedimentary basins, in *Tectonics of Sedimentary Basins: Recent Advances*, C. Busby, A. Azor, Eds. (Wiley-Blackwell, 2012), pp.111–130.
40. D. J. Jerolmack, C. Paola, Shredding of environmental signals by sediment transport. *Geophys. Res. Lett.* **37**, L19401 (2010).
41. D. J. Dunlop, Ö. Özdemir, *Rock Magnetism: Fundamentals and Frontiers* (Cambridge Univ. Press, 1997).
42. Q. Liu, C. Deng, Y. Yu, J. Torrent, M. J. Jackson, S. K. Banerjee, R. Zhu, Temperature dependence of magnetic susceptibility in an argon environment: Implications for pedogenesis of Chinese loess/palaeosols. *Geophys. J. Int.* **161**, 102–112 (2005).
43. C. Deng, R. Zhu, M. J. Jackson, K. L. Verosub, M. J. Singer, Variability of the temperature-dependent susceptibility of the Holocene eolian deposits in the Chinese loess plateau: A pedogenesis indicator. *Phys. Chem. Earth, Part A: Solid Earth Geodesy* **26**, 873–878 (2001).
44. D. Jordanova, N. Jordanova, Magnetic characteristics of different soil types from Bulgaria. *Studia Geophysica Geodaetica* **43**, 303–318 (1999).
45. R. Day, M. Fuller, V. A. Schmidt, Hysteresis properties of titanomagnetites: Grain-size and compositional dependence. *Phys. Earth Planet. Interiors* **13**, 260–267 (1977).
46. D. J. Dunlop, Theory and application of the Day plot (M_{rs}/M_s versus H_{cr}/H_c) 1. Theoretical curves and tests using titanomagnetite data. *J. Geophys. Res.* **107**, EPM 4-1–EPM 4-22 (2002).

Acknowledgments: We thank W. Xia and P. Zhang for help in sample collection and measurements. **Funding:** This work was funded by the 2nd Tibetan Plateau Scientific Expedition and Research (2019QZKK0707) and CAS programs (QYZDJ-SSW-DQC033, XDA2007010202, and 132B61KYSB20170008) grants to Z.J. and SKLLQG grant (SKLLQGPY1603) to F.Z. **Author contributions:** Z.J. and F.Z. designed and managed the project and measured the XRF. Z.J., F.Z., A.J.W., Z.A., R.G.H., and A.L.D. developed the interpretations and wrote the manuscript with help from all other authors. X.Q. and X.X. measured the magnetic minerology. Y.S. and X.L. measured the grain size and helped on data interpretation. All authors commented on the manuscript. **Competing interests:** The authors declare that they have no competing interests. **Data and materials availability:** All data needed to evaluate the conclusions in the paper are present in the paper and/or the Supplementary Materials. Additional data used in the paper are freely available from the respective websites hosting the datasets. Other data related to this paper may be requested from the authors.

Submitted 12 October 2018
Accepted 9 May 2019
Published 12 June 2019
10.1126/sciadv.aav7110

Citation: F. Zhang, Z. Jin, A. J. West, Z. An, R. G. Hilton, J. Wang, G. Li, A. L. Densmore, J. Yu, X. Qiang, Y. Sun, L. Li, L. Gou, Y. Xu, X. Xu, X. Liu, Y. Pan, C.-F. You, Monsoonal control on a delayed response of sedimentation to the 2008 Wenchuan earthquake. *Sci. Adv.* **5**, eaav7110 (2019).